

Reduction of vanadium(V) in a microbial fuel cell: V(IV) Migration and Electron Transfer Mechanism

Yuan Wang¹, Yali Feng¹, Haoran Li^{2,*}, Chaorui Yang¹, Juntong Shi³

¹ School of Civil and Resource Engineering, University of Science and Technology Beijing, Beijing 100083, China;

² State Key State Laboratory of Biochemical Engineering, Institute of Process Engineering, Chinese Academy of Sciences, Beijing 100190, China;

³ Beijing National Day School, Beijing 100039, China;

*E-mail: hrli@ipe.ac.cn

Received: 5 July 2018 / Accepted: 27 August 2018 / Published: 1 October 2018

The effects of vanadium on the microbial fuel cell performance, migration and distribution of V(IV) as well as electron transfer mechanism of single-chamber MFC were investigated by SEM, Fourier Transform Infrared Spectroscopy (FTIR), Cyclic Voltammetry (CV) and Electrochemical Impedance Spectroscopy (EIS). With anolyte vanadium concentration of 100 mg/L, the shortest degradation cycle was 130.67 h, while the degradation rate was 99.44%. V(V) combined with hydroxyl and carboxyl groups to form V(IV) organic participates, part of which deposited on the anode surface, and the other part distributed in anolyte. V(V) around cathode was reduced to V(IV) receiving electrons from the anode, meanwhile V(V) in anolyte was reduced to V(IV) owing to the electrons transfer on membrane binding enzyme complex. V(V) participated in cathode reactions instead of oxygen, accelerating the synchronization and integrity of electrode reactions.

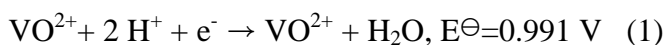
Keywords: microbial fuel cell; vanadium-containing wastewater; anode adsorption; membrane binding enzyme; V(IV) complex

1. INTRODUCTION

Microbial fuel cell(MFC) is a device that uses bacteria as catalysts to oxidize organic or inorganic matter and generate electricity, which can be used to treat certain organic wastewater and high-priced metal wastewater [1,2]. MFC serves various advantages which include wide source of fuel, mild reaction conditions, good biocompatibility, and high efficiency in electricity-generation free of pollution [3]. Based on the double-chamber MFC, single-chamber air cathode MFC, exchange Membrane-less MFC, mixed bacteria electricity-generation MFC and other new configurations have been developed [4,5,6]. Vanadium is required by human body as a trace nutrient, but it becomes toxic at high concentration [7]. The toxicity of vanadium aggravates with its valence state and solubility

[8,9,10]. V(V) is the most toxic among vanadium ions of various valence states [11,12]. In toxic waters the dominant vanadium species are the V(V) compounds [13]. The reduction of V(V) to V(IV) represents a major way to alleviate the impact of vanadium on living systems[14]. Physical and chemical methods are usually adopted to treat V(V) wastewater with a vanadium concentration of 40~110 mg/L. However, the cost-effectiveness of such methods is questionable.

Biological treatment has recently aroused much attention as a new approach to manage wastewater. Haoran et al. [15,16] utilized double-chamber MFC to reduce V(V) to low toxicity V(IV), as equation (1). It was suggested that appropriate amount of vanadium elements can promote the growth of a microorganism, and NaVO₃ anode catalyst can increase anode potential [17]. However, only few studies have reported the reduction of V(V) in single-chamber MFC. Thus, further investigations of V(V) reduction in single-chamber MFC are needed. In such a case, MFC electricity-generation characteristics and electron transfer mechanism during the reduction of V(V) by single chamber MFC were studied. Additionally, the transformation of V(V) and the distribution of reduction product V(IV) were also discussed. The study has important implications for remediation of vanadium-contaminated water bodies and the degradation and recovery of heavy metals.



2. EXPERIMENTAL METHOD

2.1 MFC fundamental structure

Single-chamber MFC consisted of two glass cylinders with a different diameter as shown in Fig. 1. The total volume of the MFC was 419 mL. Three round graphite felts with a diameter of 6.5 cm were piled in anode as an electrode, while a single layer round graphite with a diameter of 10.5 cm was adopted in the cathode. The graphite felt fiber was designed with diameter of 15 μm , thickness of 4 mm, pore size of 100 to 200 μm , specific area of 0.47 $\text{m}^2 \cdot \text{g}^{-1}$. Cathode and anode were connected by titanium wire with the external resistance of 515 Ω because excessive small external resistance was detrimental to stable operation for MFC [18]. Control group was identical to the experimental group but without external resistance. All the experiments were carried out at room temperature (30 ± 2 $^\circ\text{C}$). All tests were conducted at least in duplicate, and all statistical analyses were performed by Origin Pro 8.5.

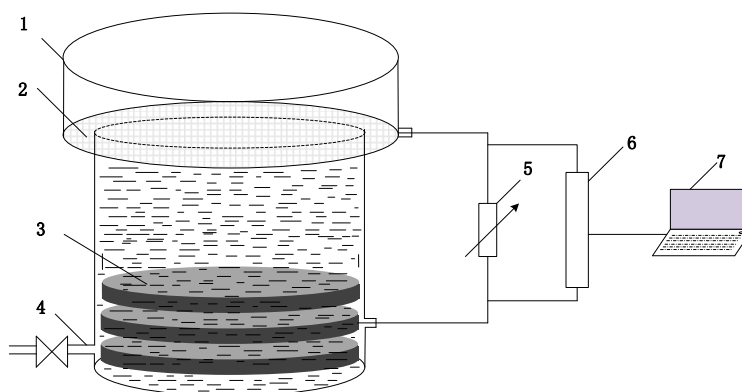


Figure 1. Diagram of single chamber membrane-less MFC

1. glass shell 2. cathode 3. anode 4. outlet valve 5. resistance box 6. data record 7. computer

2.2 samples and inoculum

The anolyte contained following components (per L): 0.13 g of KCL, 3.31 g of $\text{NaH}_2\text{PO}_4 \cdot 2\text{H}_2\text{O}$, 10.31 g of $\text{Na}_2\text{HPO}_4 \cdot 12\text{H}_2\text{O}$, 2.9 g of NaCl, 0.31 g of NH_4Cl , 10 mL of Wolfe Vitamin Solution, 10 mL of Wolfe Mineral Solution. 20 mmol/L CH_3COONa was added when MFC finished a cycle. V(V) was added into the above solution in the form of NaVO_3 with 200mg/L.

2.3 Testing and calculation

2.3.1 Electrochemical measurements

MFC output voltage data across the cell was recorded by a data acquisition system (AD8233H, Ribohua, China) at an interval of 5 min. Current density and power density were calculated according to formula (2), (3).

$$I_d = U/RA \quad (2)$$

$$P_d = U^2/RA \quad (3)$$

Where I_d is the current density; U is the output voltage; R is the external resistance; P_d is the power density; A is the anode area.

Cyclic Voltammetry (CV) and Electrochemical Impedance Spectroscopy (EIS) were tested by electrochemical workstations (CHI660D, CH Instrument Ins, China). CV was performed in a three-electrode setup comprising a glassy carbon as a working electrode, a platinum foil as an auxiliary electrode and saturated calomel electrode as the reference electrode. CV of following solution were performed with scanning speed of 25 mV/s [19]: (1) the prepared V(V) solution; (2) anolyte of MFC after substrate has been degraded completely without V(V) added; (3) filtrate of (2) with 0.22 μm filter membrane; (4) anolyte of MFC after substrate has been degraded completely with V(V) added; (5) the prepared vanadium-containing anolyte.

EIS was conducted in a frequency range of 0.005~100 KHz with an AC signal of 10 mV amplitude. Cathode or anode was used as working electrode, and the other electrode was used as the auxiliary electrode. Saturated calomel electrode was used as reference electrode. The data were fitted and simulated using Zview software based on a predetermined equivalent electrical circuit. After the first and second addition of vanadium, EIS was tested with 100 mV/s scanning speed.

2.3.2 Infrared Spectroscopy analysis

Infrared Spectroscopy: Fourier Transform infrared spectroscopy (FTIR) (ALPHA, BRUKER, Germany) was used to analyze the material changes of the bacterial membrane in vanadium-containing MFC and vanadium-free MFC. OPUS 5.0 software was applied to process the data.

2.3.3 Vanadium concentration measurements

Vanadium concentration in anolyte: Concentrations of Vanadium ions in each valence state and total vanadium were tested by potentiometric titration (ZDJ-4A, Leici, China) at the end of each cycle [20].

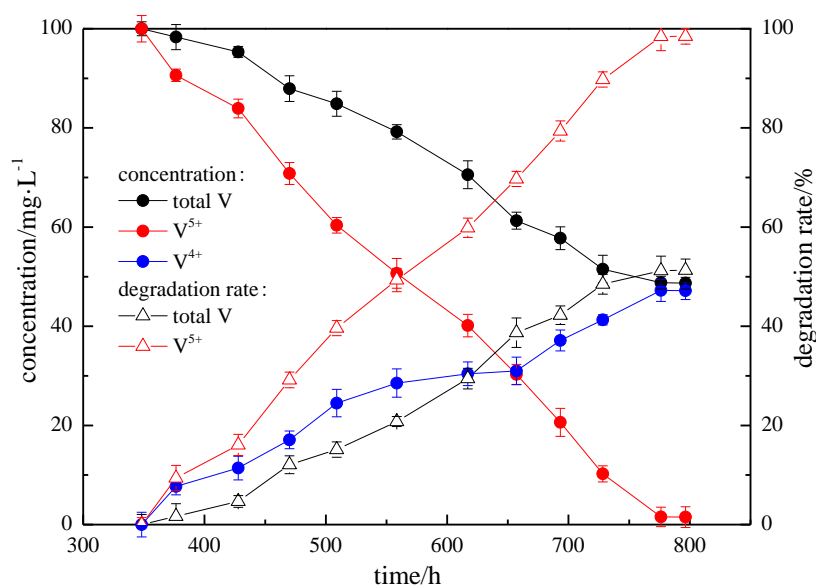
Vanadium concentration adsorbed in anodic graphite felt: Cutting 1 cm² graphite, then put it into appropriate amount H₂SO₄ (1+1). The graphite was heated in water-bath for 30 min at 80 °C. The final pH of the medium was adjusted to 7.0 and the capacity was set to 50 mL. The amount of vanadium adsorbed on the graphite felt can be calculated.

3. RESULTS AND DISCUSSION

3.1 Start-up and operation of MFC

The degradation effect of the MFC experimental group and control group was compared in terms of output voltage and V(V) degradation rate. Fig. 2 clearly showed that performance of the experimental set excelled control set. Only data of the experimental set were discussed.

Bacteria liquid were inoculated into the membrane-less air cathode microbial fuel cell. After 3 cycles operation, 1/2 anolyte was replaced with 1/2 vanadium-containing anolyte for three times (point A, B, C in Fig. 3). Maximum voltage declined from 406 mV to 237 mV after primary vanadium addition. The maximum output voltage increased gradually in subsequent cycles, and the maximum voltage finally stabilized at 447mV. The same amount of organic substrate was added each cycle, but the MFC operating cycle was shortened and the maximum output voltage was on the rise.



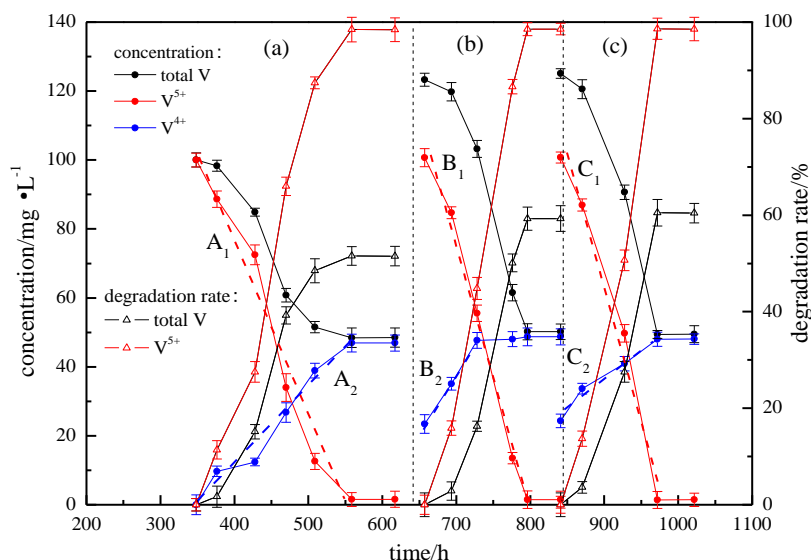


Figure 2. Concentration and degradation rate of vanadium in each valence state in MFC anolyte for control group (upper) and experimental group (lower): (a) primary V(V) addition ; (b) secondary V(V) addition ; (c) tertiary V(V) addition

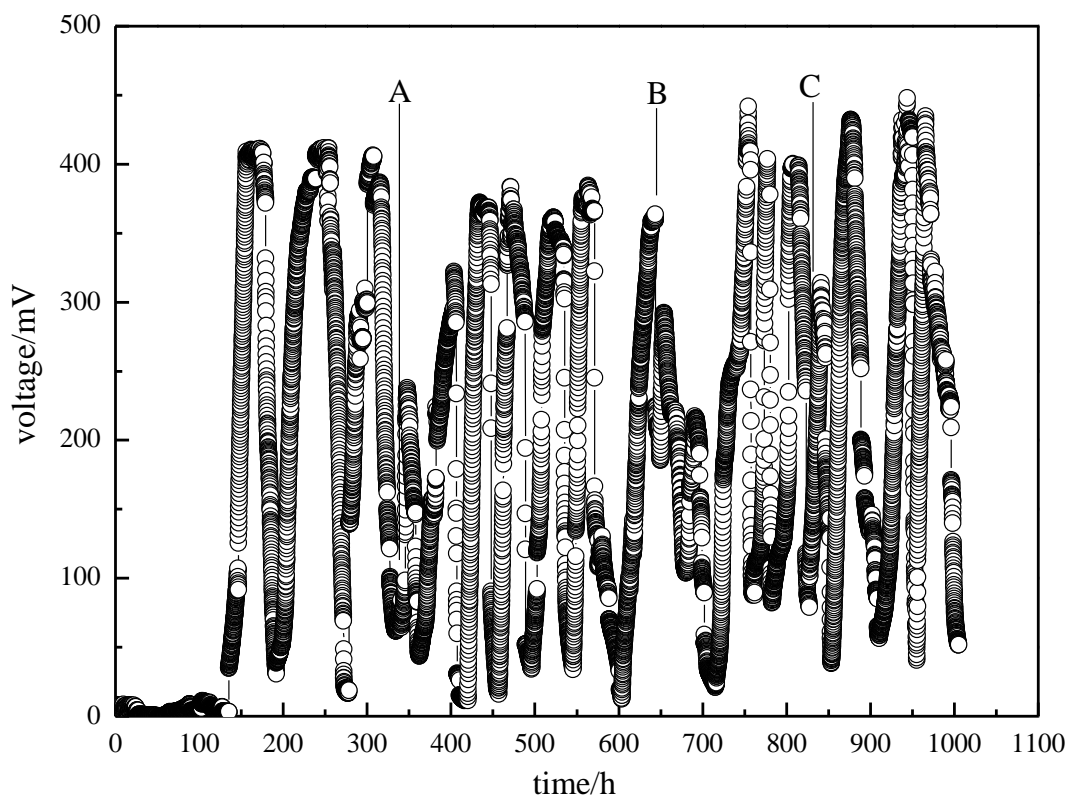


Figure 3. Graph of MFC output voltage

CH₃COONa can be regarded as an electron donor while O₂ as the electron acceptor before point A in Fig. 3. When 1/2 vanadium-containing anolyte was replaced, the microorganism in MFC

adapted gradually to the vanadium-containing anolyte with V(V) concentration of 100 mg/L. At this stage, O₂ and V(V) acted as an electron acceptor while CH₃COONa acted as an electron donor. As a result, the system can resist external shocks to ensure stable operation.

3.2 conversion and transformation of V(V) in MFC

Membrane-less air cathode MFC was constructed and operated for about 870 h. Concentrations of vanadium in each valence state in the anolyte and anodic graphite felt were shown in Table 1.

Table 1. Vanadium concentrations in anolyte and anode graphite felt of each cycle

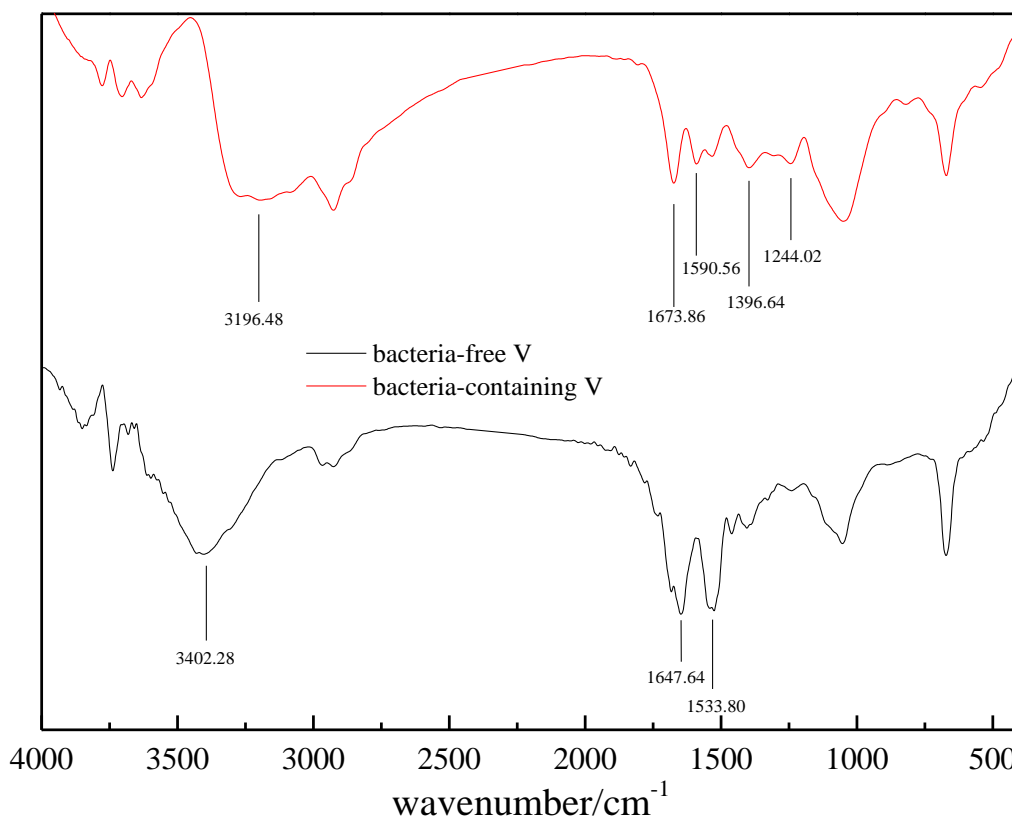
Cycle	vanadium addition/mg	anolyteV(V) /mg·L ⁻¹	anolyteV(IV) /mg·L ⁻¹	anodic adsorption of V ⁴⁺ /mg	MFC total vanadium /mg
1	non	0	0	0	0
2	41.90	88.62	9.70	0.70	41.90
3	non	72.48	12.39	6.34	41.90
4	non	34.01	26.75	16.44	41.90
5	non	12.59	38.93	20.31	41.90
6	non	1.55	46.90	21.60	41.90
7	41.90	84.69	35.10	23.06	73.25
8	non	55.53	47.70	30.00	73.25
9	non	13.48	48.03	47.48	73.25
10	non	1.47	48.73	52.22	73.25
11	41.90	86.94	33.64	54.11	104.63
12	non	49.71	40.95	66.65	104.64
13	non	1.40	48.01	83.93	104.63

V(V) was added to anolyte until the concentration of V(V) remained stable. Linear fitting of V(V) and V(IV) concentrations was performed at this time interval. Then, the slope absolute value of the fitted line represented the degradation rate of V(V) and formation rate of V(IV). After three times the addition of V(V), linear fitting lines of V(V) and V(IV) concentration were A₁, A₂, B₁, B₂, C₁ and C₂ respectively. Linear fitting data were shown in Table 2. From Table 2, the degradation rates of V(V) were 0.5079, 0.7485, 0.7511, however, the formation rates of V(IV) were 0.2244, 0.3406, 0.1706 respectively after adding V(V) for three times. The result showed that the formation rate of V(IV) was much lower than the degradation rate of V(V) in anolyte. It can be assumed that part of V(IV) was adsorbed on the anode graphite felt. At the same time, the sum of vanadium concentration in anolyte and anode graphite felt was approximately equal to the theoretical value of vanadium concentration (41.9 mg, 73.75 mg, 103.70 mg), demonstrating that the reduction product of V(V) distributed mainly in anolyte and anode graphite felt. The V(V) degradation rates increased gradually, which were 98.45%, 99.16%, and 99.44% respectively.

Table 2. Data of linear fitting line

	Equation	R ²
A ₁	y=-0.5079x+279.24	0.9693
A ₂	y=0.2244x-78.174	0.9701
B ₁	y=-0.7485x+597.73	0.9892
B ₂	y=0.3406x-200.59	0.999
C ₁	y=-0.7511x+737.65	0.9746
C ₂	y=0.1706x-117.25	0.9683

From Fig. 4, 3402.28 cm⁻¹ was a vibration absorption peak for the -OH of carbohydrate [21], and the peak widened and shifted to 3196.48 cm⁻¹ after V(V) added, proving that the -OH of carbohydrate molecules were involved in pairing. 1647 cm⁻¹, 1533 cm⁻¹ were absorption peaks for -COOH [21], and the absorption peak intensity was weakened after V(V) added. 1396 cm⁻¹, 1244 cm⁻¹ were antisymmetric and symmetrical stretching vibration peaks of COO [21], indicating that -COOH was involved in pairing. V(IV) was able to combine with organic molecules [10], and it was more stable for VO²⁺ combined with hydroxyl group and carboxyl group at the same time [22]. Therefore, in the MFC system, V(V) was reduced to V(IV), and V(IV) combined with microorganisms and their secreted organic matter to form VO²⁺ participates. The composition was similar to that of the precipitates observed in a previously published vanadate bioreduction study [7,14]. Some of V(IV) participates distributed in anolyte, and some of them were adsorbed by anodic graphite felt.

**Figure 4.** Infrared spectra of anodic biofilm before and after vanadium addition

3.3 effect of $V(V)$ on MFC internal resistance

Output voltage polarization and power density of MFC without adding vanadium, adding vanadium at the first time and the second time were shown in Fig. 5(a). Output power density reached its maximum when the external resistance was equal to the apparent internal resistance. It is indicated that the apparent internal resistance increases in the MFC system because power density reduces sharply after vanadium added.

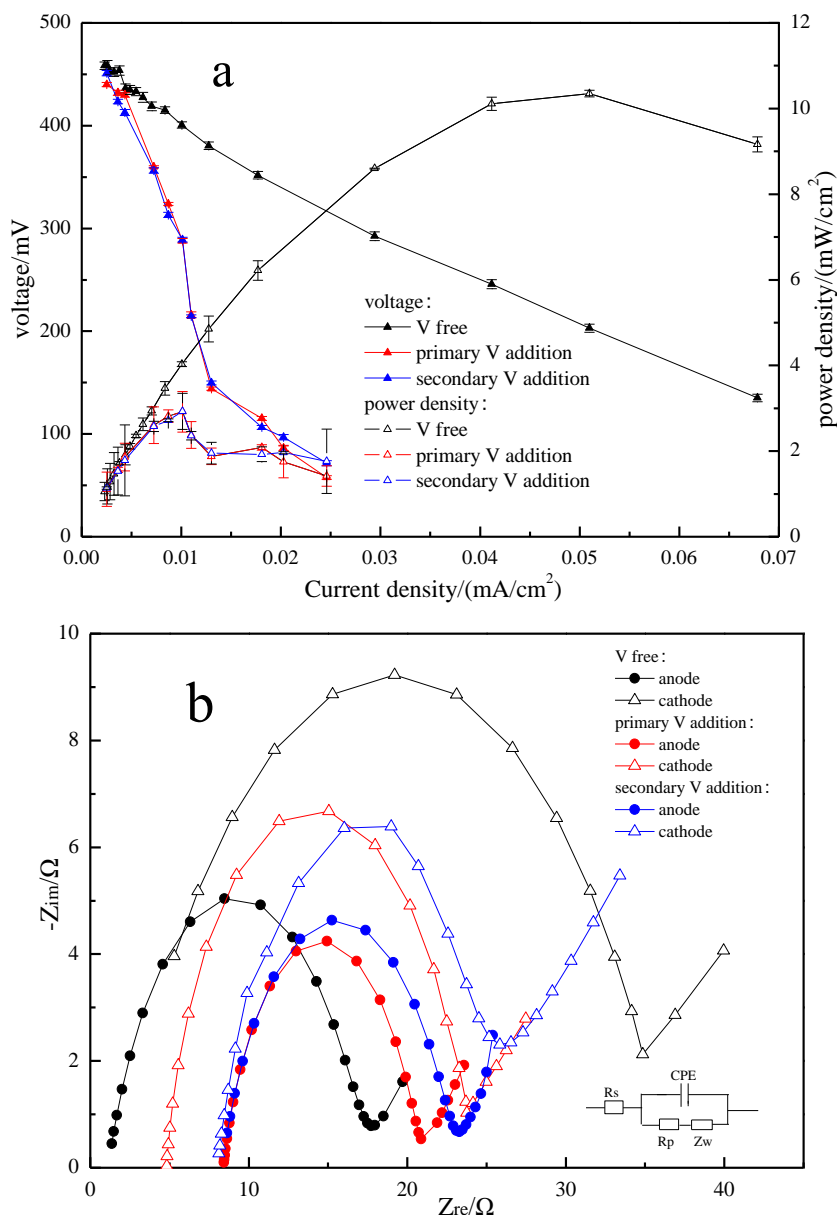


Figure 5. Output voltage polarization and power density of MFC (a) MFC power density and polarization curves; (b) EIS of MFC cathode and anode

From EIS of cathode and anode (Fig. 5(b)), apparent internal resistance (the sum of anode, cathode polarization resistance and total ohm internal resistance) were 60 Ω, 280 Ω, 290 Ω and 290 Ω respectively before and after 1/2 replacement of vanadium-containing anolyte. The total ohmic resistance (the sum of the internal resistance of the cathode, anode, and anolyte) were 10.64 Ω, 248.35

Ω , 257.46 Ω and 257.75 Ω respectively, suggesting the ohmic resistance of MFC system increased dramatically.

It can be seen from Fig. 5(b) and Table 3 that the anodic polarization resistance decreased from 16.77 Ω to 12.79 Ω , 14.32 Ω , and 15.09 Ω , and the cathodic polarization resistance decreased from 32.59 Ω to 18.86 Ω , 18.22 Ω and 18.02 Ω after vanadium added. It was shown that the anodic polarization resistance decreases with the addition of V(V), and the oxidation-reduction rate increased [23,24]. The cathodic polarization resistance of the MFC system reduced significantly, resulting in the cathodic shielding effect of the electrochemical reaction on MFC system reduced obviously.

Table 3. The internal resistance of MFC before and after adding V(V)

		non	Primary addition	Secondary addition	Tertiary addition
ohmic resistance/ Ω	anode	1.23	8.41	8.57	8.54
	cathode	2.74	4.9	8.09	9.21
	anolyte	6.67	235.04	240.8	240
Polarization resistance/ Ω	anode	16.77	12.79	14.32	15.09
	cathode	32.59	18.86	18.22	18.02
MFC apparent internal resistance / Ω		60	280	290	290

3.4 Analysis of electron transfer path in MFC vanadium degradation

From CV of V(V)-containing solution(Fig. 6(a)), A, B, C, D, E, F represent reduction potentials of V(V) to V(IV), V(IV) to V(III), V(III) to V(II), oxidizing potentials of V(II) to V(III), V(III) to V(IV) and V(IV) to V(V) corresponding [25,26].

CV of V(V)-containing anolyte before and after MFC processing is shown in Fig. 6(b). A, A' is the reduction peak of V(V) to V(IV), and B, B' is the oxidation peak of V(IV) to V(V). Positive shift in oxidation peak and reduction peak was observed for vanadium-containing anolyte after MFC treatment. With a positive shift of V(IV) oxidizing potential and a negative shift of V(V) reduction potential, we can draw a conclusion that V(V) is easier reduced to V(IV) while V(IV) is more difficult oxidized to V(V) under the catalyst of microorganisms.

CV of vanadium-containing anolyte before and after filtering by 0.22 μm filter membrane was shown as Fig. 6(c). CV of vanadium-containing anolyte after filtering by 0.22 μm filter membrane was smoother, and no redox peak was observed. The result proved that the redox material attached to the bacteria was filtered out. SEM of the anolyte filter and anode graphite felt was shown in Fig. 7. A large number of bacteria attached to the anode graphite felt (Fig. 7(a)), forming a biofilm (Fig. 7(b)). V(IV) precipitates accumulated on surface of the biofilm (Fig. 7(c)). After adding vanadium, the quantity of microorganisms (Fig. 7(d)) and V(IV) precipitates (Fig. 7(e)) in the anode filter increased significantly.

Many researchers have proposed electron transfer mechanisms for MFC [27,28,29]: (1) Direct electron transfer is achieved via cell membrane binding enzyme complex or nanowires[30, 31]; (2) Indirect electron transfer via electron shuttles or mediators [32,33,34,35,36]. Indirect electron transfer

means organic or inorganic soluble compounds are reduced or oxidized in the cell and then react with insoluble electron acceptors or donors [37]. And there are two mechanisms for V(V) reduction by microbes: intracellular [38] and membrane-associated [39] V(V) reduction. In the intracellular reduction model, through the phosphate transport system into the cell [40], vanadate oxyanion is reduced by high concentrations of intracellular reducing agents. In such a case, a small quantity of vanadium may remain in the cell. On the contrary, the membrane associated bioreduction model proposes that V(V) reduced to vanadyl by vanadate–reductase system embedded in the cell membrane [41,42,43,44] and no vanadium enters the cell. Fig. 6(c) showed that the substances involved in the redox reaction in the anolyte were insoluble, and nanowires were not observed in Fig. 7. Besides, results revealed that almost all the vanadium distributed in anolyte and anode graphite felt, not inside the cells (Table 1). Therefore, we concluded that V(V) bioreduction by these methanogens should be extracellular and electron in anolyte is transferred through cell membrane binding enzyme complex.

The electron transfer model in MFC is shown in Fig. 8, where (A) is around the anode. In the area, electricity-generation bacteria attached to the anode consumes CH_3COONa and produces electrons with the catalysis of membrane binding enzyme complex.

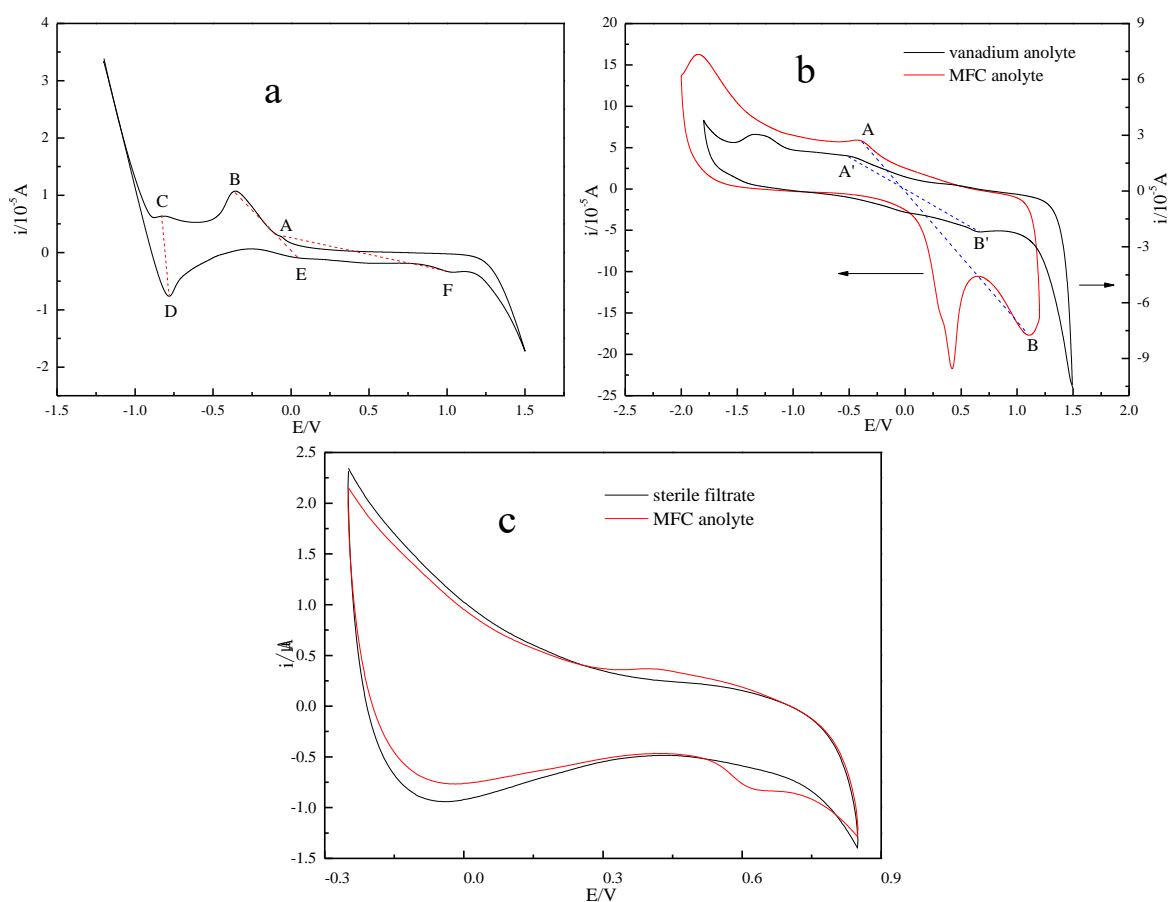


Figure 6. Cyclic Voltammetry of MFC (a) V(V) solution (scanning speed 100 mV/s) ; (b) V(V) anolyte before and after MFC treatment (scanning speed 100 mV/s); (c) anolyte before and after filtration without V(V) added (scanning speed 25 mV/s)

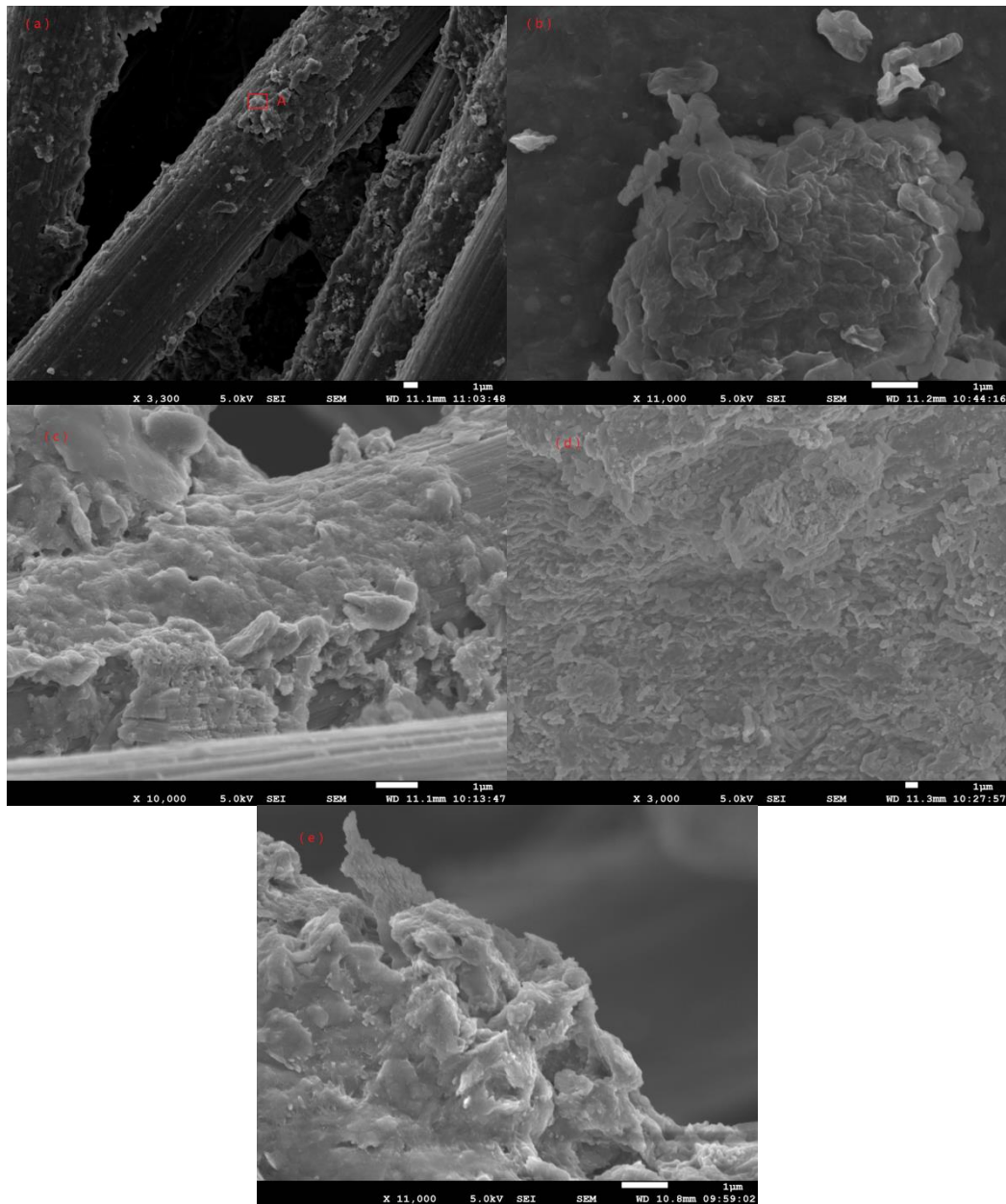


Figure 7. SEM of anolyte filter and anode graphite felt (a) anode graphite felt; (b) the amplified image of region A in Fig. (a); (c) V(IV) complex deposition on the surface of anodic graphite felt; (d) microorganism in anolyte filter; (e) anolyte filter

Electrons pass to cathode through the anode graphite felt, then V(V) is reduced to V(IV) as electron acceptor; (B) indicate that V(V) is reduced directly for accepting electrons produced by electricity-generation bacteria in the anode chamber; Besides, (C) also shows that O₂ and V(V) competed for electrons.

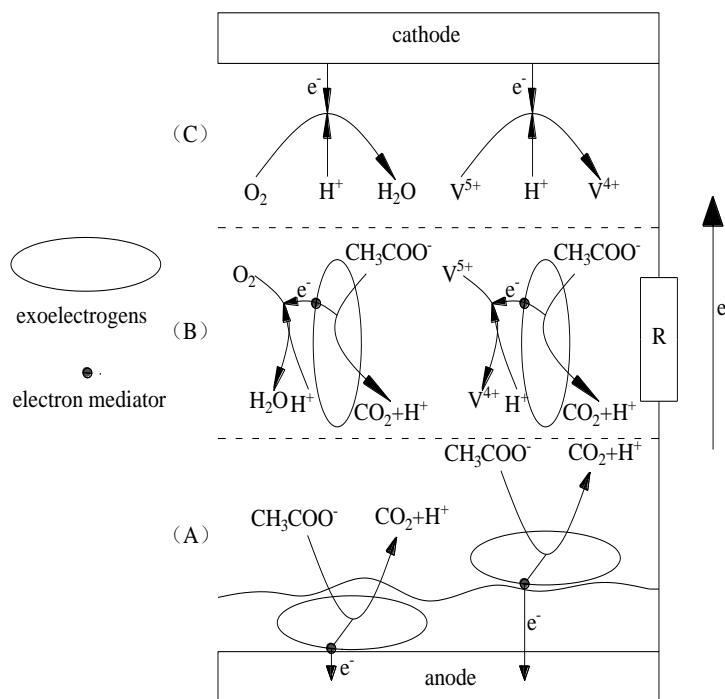


Figure 8. Electron transfer model

4. CONCLUSIONS

(1) single-chamber MFC is able to reduce V(V) and generate electricity. With anolyte vanadium concentration of 100 mg/L, the shortest degradation cycle was 130.67 h, and the degradation rate was 99.44%. The voltage maximum dropped from 406 mV to 384 mV after vanadium addition and the voltage maximum rose to 447 mV subsequently because the microorganism adapts to the vanadium-containing anolyte gradually and the MFC tends to be steady-going. After adding V(V) into MFC, anode and cathode polarization resistances decreased and oxidation-reduction reaction rates increased. V(V) participate in cathode reaction, accelerating the synchronization and integrity of cathode and anode reaction. In addition, the reduction of V(V) is easier achieved in the MFC system.

(2) The electron transfer path for MFC V(V) reduction is as follows: Bacteria consumed organic matter to generate electrons, and part of the electrons passed to the cathode through the anode. Accepting electrons from the cathode, V(V) is reduced to V(IV). Additionally, electron transfer through membrane binding enzyme complex on the microbial cell membrane in anolyte. As a result, V(V) bioreduction occur extracellularly.

(3) V(V) in MFC anolyte is reduced to V(IV) as electron acceptor. V(IV) combine with microorganism and hydroxyl, carboxyl groups to form V(IV) organic participates, enriching in the anolyte or anode. The formation of V(IV) participates in anolyte result in an increase of total ohmic resistance and total vanadium content dramatically; V(IV) participates adsorb on anode surface and increase gradually with the MFC running.

ACKNOWLEDGEMENTS

This research was supported by the Major Science and Technology Program for Water Pollution Control and Treatment[No. 2015ZX07205-003]; China Ocean Mineral Resources Research & Development Program[No. DY125-15-T-08], and the National Natural Science Foundation of China[No. 21176026, 21176242].

References

1. J. Lian, X. Tian, J. Guo, Y. Guo, Y. Song, L. Yue, Y. Wang, X. Liang, *Biochem. Eng. J.*, 114 (2016) 167.
2. Z. Liu, J. Liu, S. Zhang, Z. Su, *Biochem. Eng. J.*, 45 (2009) 185.
3. A. Ebrahimi, D.Y. Kebria, G.N. Darzi, *Water Sci. Technol.*, 76 (2017) 1206.
4. S. Ayyaru, S. Dharmalingam, *Anal. Chim. Acta*, 818 (2014) 15.
5. C. Santoro, I. Ieropoulos, J. Greenman, P. Cristiani, T. Vadas, A. Mackay, B. Li, *J. Power Sources*, 238 (2013) 190.
6. G. Wang, L. Wei, C. Cao, M. Su, J. Shen, *Int. J. Hydrogen Energy*, 42 (2017) 11614.
7. J. Zhang, H. Dong, L. Zhao, R. Mccarricket, A. Agrawal, *Chem. Geol.*, 370 (2014) 29.
8. J. L. Domingo, J. M. Llobet, J. Corbella, *Toxicol. Lett.*, 26 (1985) 95.
9. B. R. Nechay, *Annu. Rev. Pharmacol. Toxicol.*, 24 (2008) 501.
10. M. S. Patole, T. Ramasarma, *J. Neurochem.*, 51 (2010) 491.
11. A. Safavi, H. Abdollahi, F. Sedaghatpour, S. Zeinali, *Anal. Chim. Acta*, 409 (2000) 275.
12. L. J. Alemany, M. A. Larrubia, J. M. Blasco, *Fuel.*, 77 (2014) 1735.
13. L. Minelli, E. Veschetti, S. Giammanco, G. Mancini, M. Ottaviani, *Microchem. J.*, 67 (2000) 83.
14. I. Ortizbernad, R.T. Anderson, H. A. Vrionis, D. Lovley, *Appl. Environ. Microbiol.*, 70 (2004) 3091.
15. C. Zheng, H. Zhang, B. Zhang, P. Li, H. Xu, *Environ. Prot. Chem. Ind.*, 35 (2015) 247.
16. H. Li, Y. Feng, X. Zou, X. Luo, *Chin. J. of Nonferrous Met.*, 9 (2009) 1700.
17. S. Li, Z. Du, X. Zhu, W. Liu, D. Fu, H. Li, *Chin. J. Process Eng.*, 7 (2007) 589.
18. D. Chang, Z. Lu, C. Wu, Y. Chen, L. Cai, L. Zhang, *Chin. J. Environ. Eng.*, 9 (2015) 5113.
19. Y. Yin, *Basic study on the Electricity Generation Process and Performance Optimization of Two-chamber Mediator-less Microbial Fuel Cell*, East China University of Science and Technology, (2013) Shanghai, China.
20. H. Ren, H. Zhao, Y. Chun, C. Ma, *Phys. Test. Chem. Anal., Part B*, 52 (2016) 853.
21. J. Feng, *Application of infrared spectroscopy in trace evidence analysis*, Chemical Industry Press, (2010) Beijing, China.
22. Z. Gao, *Study on the Complexation of Vanadium Ions with the Tannin Extract*, Taiyuan University of Technology, (2013) Shanxi, China.
23. C. Zhang, *Study on Vanadium Accumulation and some biochemical characteristics of*

Saccharomyces cerevisia, Anhui Agricultural University, (2005) Anhui, China.

24. S. Srikanth, E. Marsili, M.C. Flickinger, D.R. Bond, *Biotechnol. Bioeng.*, 99 (2010) 1065.
25. Y. Liu, H. Liu, X. Xia, *Electrochemistry*, 8 (2002) 40.
26. E. Sum, M. Rychcik, M. Skyllas-Kazacos, *J. Power Sources*, 16 (1985) 85.
27. R. Kumar, L. Singh, A.W. Zularisam, *Renewable Sustainable Energy Rev.*, 56 (2016) 1322.
28. L. Huang, J.M. Regan, X. Quan, *Bioresour. Technol.*, 102 (2011) 316.
29. D.R. Lovley, *Curr. Opin. Biotechnol.*, 17 (2006) 327.
30. N.S. Malvankar, S.E. Yalcin, M.T. Tuominen, D.R. Lovley, *Nat. Nanotechnol.*, 9 (2014) 1012.
31. J. Yun, N.S. Malvankar, T. Ueki, D.R. Lovley, *Isme J.*, 10 (2016) 310.
32. Y. Hubenova, M. Mitov, *Bioelectrochemistry*, 106 (2015) 232.
33. M.R. Miroliaei, A. Samimi, D. Mohebbi-Kalhari, M. Khorram, *J. Ind. Eng. Chem.*, 25 (2015) 42.
34. Y. Qiao, Y. Qiao, L. Zou, C. Ma, J. Liu, *Bioresour. Technol.*, 198 (2015) 1.
35. H. Von Canstein, J. Ogawa, S. Shimizu, J.R. Lloyd, *Appl. Environ. Microbiol.*, 74 (2008) 615.
36. S. Xu, Y. Jangir, M.Y. El-Naggar, *Electrochim. Acta.*, 198 (2016) 49.
37. K. Rabaey, J. Rodríguez, L.L. Blackall, J. Keller, P. Gross, D. Batstone, W. Verstraete, K.H. Nealon, *Isme J.*, 1 (2007) 9.
38. G.R. Willsky, D.A. White, B.C. McCabe, *J. Biol. Chem.*, 259 (1984) 13273.
39. M.J. Van, D.J. Opperman, L.A. Piater, E. V. Heerden, *Biotechnol. Lett.*, 31 (2009) 845.
40. B.J. Bowman, *J. Bacteriol.*, 153 (1983) 286.
41. L. Bisconti, M. Pepi, S. Mangani, F. Baldi, *Biometals*, 10 (1997) 239.
42. J.M. Myers, W.E. Antholine, C.R. Myers, *Appl. Environ. Microbiol.*, 70 (2004) 1405.
43. W. Carpentier, L.D. Smet, J.V. Beeumen, A. Brige, *J. Bacteriol.*, 187 (2005) 3293.
44. M.J. Van, D.J. Opperman, L.A. Piater, H.E. Van, *Biotechnol. Lett.*, 31 (2009) 845.